sustainability

MDPI

Article

An Experimental and Modeling Study on the Effect of Wall Opening Location on the Under-Ventilated Compartment Fire

Lujia Wang [1] and Haejun Park [2,*]

[1] HDR Inc., Charlotte, NC 28202, USA
[2] Fire Protection and Safety Engineering Technology, Oklahoma State University, Stillwater, OK 74075, USA
* Correspondence: haejun.park@okstate.edu; Tel.: +1-405-744-9517

Abstract: An experimental and modeling study was carried out to investigate the effect of wall opening location on the mass flow rates of gases through the opening and the associated fire phenomena, such as compartment temperature, projected flame height through the opening, and the heat release rates inside and outside the compartment. A 0.3 m by 0.3 m opening was placed at three different elevations—bottom, middle, and top—of a narrow end wall of a 0.8 m by 1.2 m by 0.8 m (H) compartment. A propane gas burner was used to provide four different fire sizes in the compartment: 90, 110, 130, and 150 kW. The existing correlations for mass flow rates and heat release rates generally do not include the wall opening location as a variable and are functions of only the opening area and height. Based on the experimental and modeling analysis, it is found that the wall opening location affects the internal and external fire phenomena. Two fundamental factors, K and O, are introduced to explain the effect quantitatively. Factor K is the ratio of the air inflow predicted by Fire Dynamics Simulator (FDS) to the existing correlation ($0.5A_o\sqrt{H_o}$), and Factor O is the ratio of the oxygen consumption rate in the compartment to the oxygen flow rate into the compartment, indicating combustion efficiency. Factor K ranges from 0.78 to 0.94, and O ranges from 0.67 to 0.85 for different opening locations, which suggests that the existing correlations may overestimate the amount of airflow to and the combustion efficiency within the compartment.

Keywords: compartment fire; under-ventilated; external flame; FDS modeling; opening location

check for updates

Citation: Wang, L.; Park, H. An Experimental and Modeling Study on the Effect of Wall Opening Location on the Under-Ventilated Compartment Fire. *Sustainability* **2022**, *14*, 12084. https://doi.org/10.3390/su141912084

Academic Editor: Manhou Li

Received: 23 August 2022
Accepted: 21 September 2022
Published: 24 September 2022

1. Introduction

When a fire consumes existing oxygen in a compartment, the compartment becomes fuel-rich, or under-ventilated, generating excess fuel gases [1]. If openings such as broken windows are created, unburned fuel gas leaves the compartment and generates an external flame [2,3]. This may yield a significant fire spread hazard if the flame is large enough to ignite items on the upper floors. When the upper floor becomes involved with fire, the fire from both floors may merge, leading to a larger fire [4]. This hazard has been well-recognized in the fire research field, and various studies regarding this issue have been conducted since the 1960s. To quantify this hazard, correlations for external flame heights [5,6] and the resulting irradiance on the upper wall surface [3,7–9] have been developed to check if a spread is likely to occur. Two of the factors that influence the severity of the external flame are the airflow rate into the compartment through the openings and the fuel gas generation rate in the compartment. A brief explanation is included below.

For a compartment fire with an opening, hot gases leave the compartment through the upper part of the opening due to buoyancy, and fresh air flows into the compartment through the bottom portion of the opening, as shown in Figure 1.

The correlations for the neutral plane height (h_1) from the bottom of the opening and the mass flow rate of air into the compartment are presented, as shown in Equations (1) and (2), respectively [10].

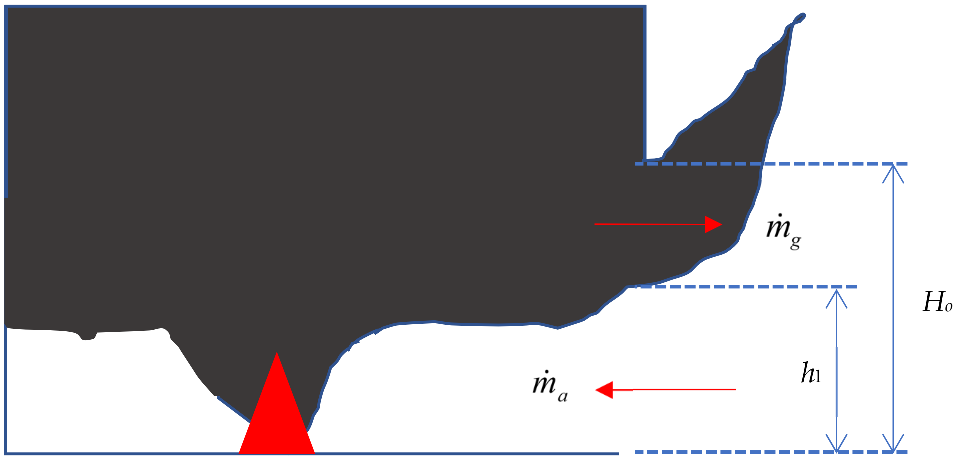

Figure 1. Compartment gas flow diagram where $\dot{m}_g$ is the mass flow rate out of the compartment and $\dot{m}_a$ is the mass flow rate into the compartment.

$$h_1 = \frac{H_o}{1 + \left(\frac{\rho_a}{\rho_g}\right)^{1/3}} \tag{1}$$

$$\dot{m}_a = \frac{2}{3} C_d W_o \rho_a \sqrt{\frac{2(\rho_a - \rho_g)g}{\rho_a}} h_1{}^{3/2} \tag{2}$$

Equation (2) is further simplified into Equation (3).

$$\dot{m}_a = \frac{2}{3} C_d A_o \sqrt{H_o} \sqrt{2g} \rho_a d_f \tag{3}$$

where:

$$d_f = \sqrt{\frac{(\rho_a - \rho_g)/\rho_a}{\left[1 + \left(\frac{\rho_a}{\rho_g}\right)^{1/3}\right]^3}}$$

Here, d_f, density factor, is the only variable that determines the amount of airflow into the compartment for a given opening configuration and ambient conditions. It becomes a maximum value of 0.214 when T_g is about 730 K (or T_g/T_a = 2.5) and slightly decreases as T_g increases. A previous study found that a representative value of 0.214 can be used for most compartment fire conditions where the temperature ratio is greater than 2, i.e., T_g above 540 K, or a relatively well-developed fire in a compartment [10]. When T_g is less than this value, e.g., at a relatively early stage of fire, the density factor is much less than 0.2. This relationship is presented in Figure 2.

With the following values: density factor = 0.214, C_d = 0.7, g = 9.81 m/s^2, ρ_a = 1.2 kg/m^3, Equation (3) turns into the well-known Equation (4).

$$\dot{m}_a \approx 0.5 A_o \sqrt{H_o} \tag{4}$$

It is often assumed that the inflow is 100% fresh air, and all the air which enters the compartment is well mixed and completely burned inside the compartment. Since burning 1 kg of air can generate about 3000 kJ energy for most fuels [11], the heat release rate (HRR) inside the compartment changes, as presented in Equation (5). Both Equations (4) and (5) have been widely applied in compartment fire research [10,12–15].

$$\dot{Q}_c = 3000 \cdot \dot{m}_a = 1500 A_o \sqrt{H_o} \tag{5}$$

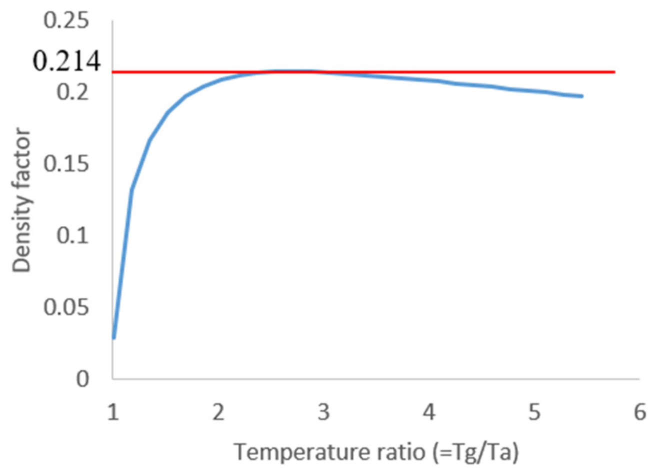

Figure 2. Density factor in Equation (3) as a function of temperature ratio (= T_g/T_a) where T_g is the upper gas layer temperature in the compartment, and T_a is the ambient temperature (=293 K).

Previous studies often used the multiplied value of the opening area and the square root of the height as a single variable, often called the ventilation factor, to determine the mass flow rate of air and the maximum HRR within the compartment. Recent studies demonstrated that other variables, such as opening shape [16–18], fuel elevation [19], and compartment size [5,20], also influence the external flame phenomena. However, these studies were conducted with a centrally located wall opening [21,22], and very limited research using the opening elevation as an independent variable exists. Frank et al. [23] investigated external flame height and incident heat flux on the exterior wall using heptane with different elevations of a wall opening and compared the results with existing correlations developed using a central opening. Lu et al. [24] developed new correlations for the external flame height using propane fuel based on the two non-dimensional length scales developed by Lee et al. [5]. They also showed that compartment temperature and external flame height increase as the opening moves from the bottom to the middle and decrease when the opening moves from the middle to the top. In addition, the heat release rate within the compartment decreases as the opening moves from the bottom to the top. These two studies accepted existing correlations, such as Equations (4) and (5), as they are, and additional terms were employed to explain variations in experimental results. The current study also investigates the effect of opening elevation on general compartment fire phenomena, such as external flame height and compartment temperature, but with a focus on the mass flow rates through the opening and the combustion efficiency within the compartment, which have not been well studied in previous research.

2. Method

Both experiments and computer modeling studies are conducted for the followings: the temperature inside the compartment, the external flame height, and the total HRR. Modeling is used to calculate the HRRs inside and outside the compartment individually, which is not possible in the experiments. Since Fire Dynamics Simulator (FDS) also allows advanced calculation devices, the mass flow rates of substances in and out of the compartment are included to investigate how the wall opening location influences the compartment fire phenomena.

2.1. Experiments

The current study used a scaled compartment that is 0.8 m wide, 1.2 m deep, and 0.8 m high, which is based on ASTM E2257 or NFPA 265, as illustrated in Figure 3. The compartment, other than the front wall, was constructed in two layers: 1.27 cm thick ceramic fiberboards were used for the inner layer, and 2.54 cm thick calcium silicate boards were installed for the outside layer. For the front wall, 0.635 cm thick cement board was used. To replicate the upper floor's exterior wall, a 0.8 wide and 1.8 m high cement board was installed right above the front wall. To reduce the uncertainty of heat feedback from the flame to the fuel surface and associated oxygen consumption in the compartment [25–27], a propane gas burner attached to a digital flow rate controller was used. The burner was located 0.4 m away from the front wall in the middle of the two side walls.

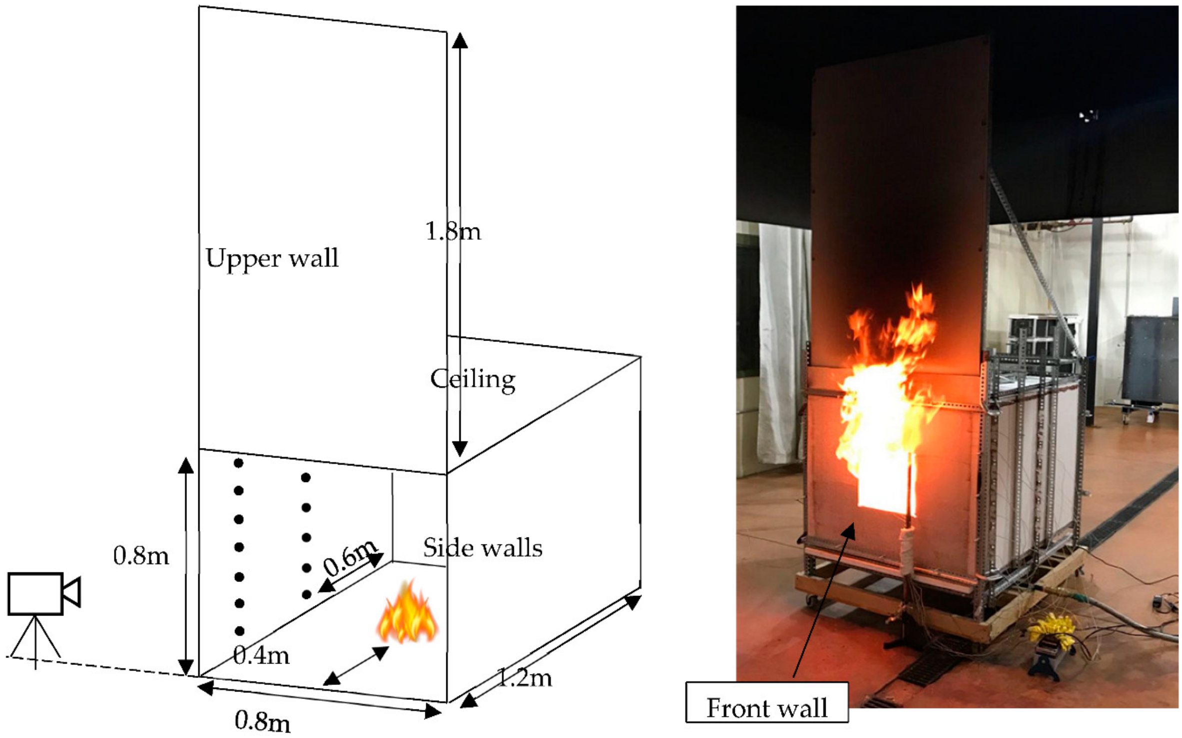

Figure 3. Compartment box configuration and device installation.

Figure 4 depicts the three different locations of the 0.3 × 0.3 m front wall opening—bottom, middle, and top. According to Equation (5), the fire size to produce an external flame need to be greater than 75 kW. In the current study, four different fire sizes were chosen—90, 110, 130, and 150 kW—within the compartment, which theoretically generate external fires of 15, 35, 55, and 75 kW, respectively.

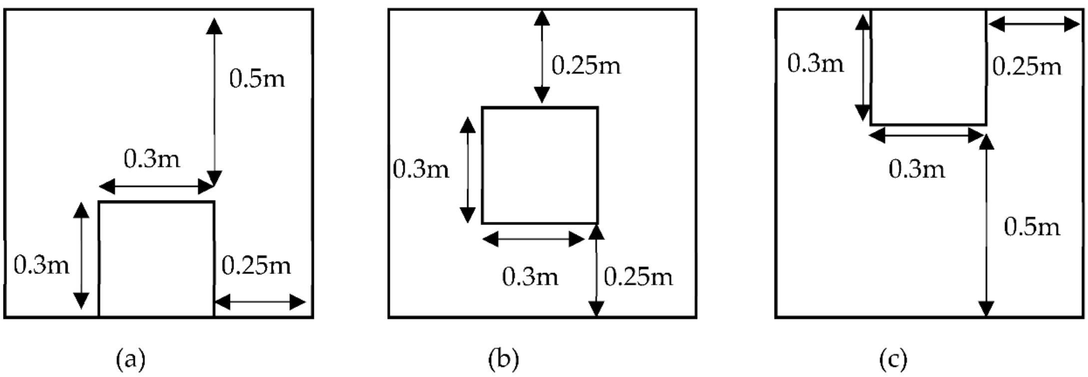

Figure 4. (**a**) Bottom, (**b**) middle, and (**c**) top openings.

The experiments were conducted in an indoor lab with the compartment located under a large exhaust hood. The initial ambient temperature and the make-up air temperature varied between 0–10 °C. The following devices were installed to measure the compartment gas temperature and the external flame height.

(a) The compartment gas temperature was measured using a total of 14 K-type thermocouples (TC), as shown in Figure 5. The front TCs and the middle TCs were 10 cm and 60 cm away from the front wall, respectively. The TC beads were located 5 cm away from the interior wall surface. As the compartment fire reaches a steady-state, the gas temperature inside the compartment also becomes relatively uniform [2,17]. For further analysis, the average value of the 14 TCs was used to represent the compartment temperature.

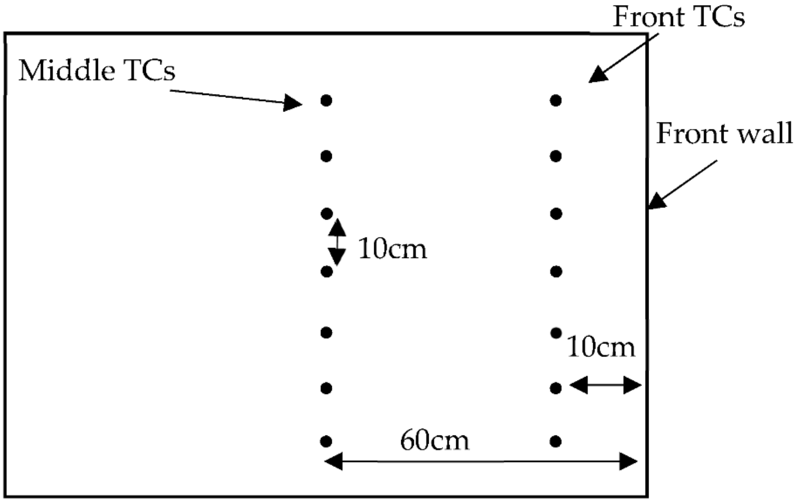

Figure 5. Thermocouple configuration on the side wall.

(b) The external flames were captured using a charged-coupled device (CCD) camera, and the flame height was calculated using an in-house MATLAB code [23]. For accurate flame region extraction, a thick black cloth was located in the background for the video data. One image per second was sampled from the video data. A threshold value to discern the flame region from the rest of the image area was first determined by the authors based on three randomly selected flame images, and all the sampled images were subjected to the threshold value. This produced black and white imaging from the videos, as shown in Figure 6. The white area shows the flame shape. The pixels between the highest white point and the lowest white point were counted at each frame and 50% intermittency was used to calculate the flame height.

(a) (b)

Figure 6. (**a**) flame image captured by a CCD camera and (**b**) flame shape extracted by a MATLAB code for a 150 kW fire.

(c) HRR was measured using an oxygen depletion calorimeter. The calorimeter was first calibrated against a propane gas flow meter at the four different fire sizes mentioned previously.

2.2. FDS Computer Modeling

FDS is a fire modeling computer program developed by NIST, and it has been widely used to study compartment fire phenomena [28]. In the current study, FDS 6.7.5 was used. The dimensions of the compartment model in FDS are identical to those of the experiments, but additional devices were located in the FDS model to assess crucial parameters that are not directly measured in the experiments.

(a) Two HRR devices were located in the FDS model, one inside ($\dot{Q}_{in}$), and the other outside ($\dot{Q}_{ex}$) the compartment. This is one of the major advantages of computer modeling, as there are no accurate means to individually measure the HRR inside and outside the compartment in experiments.

(b) In order to analyze the combustion reaction inside and outside of the compartment, substances in the inflow and the outflow through the opening need to be identified. Flow devices were located at the opening in the FDS model to calculate the bidirectional mass flow rates of the following substances: total mass flow, air, oxygen, fuel, product, CO_2, CO, N_2, water vapor, unburn fuel gas (propane), and soot.

(c) The external flame height (h_f) was determined by the heat release rate per unit length (HRRPUL) device. The HRRPUL device calculates the time-averaged heat release rate at the device height. As indicated in Figure 7, an HRRPUL device was inserted into each grid cell from the bottom of the compartment to the top of the front panel. The outputs were integrated from the bottom to the top until the integrated value reached 99% of the input HRR used for simulation and the top device's location is considered to be the flame tip location [29]. The neutral plane height was calculated based on Equation (1), and flame height was determined from the neutral plane to the flame tip.

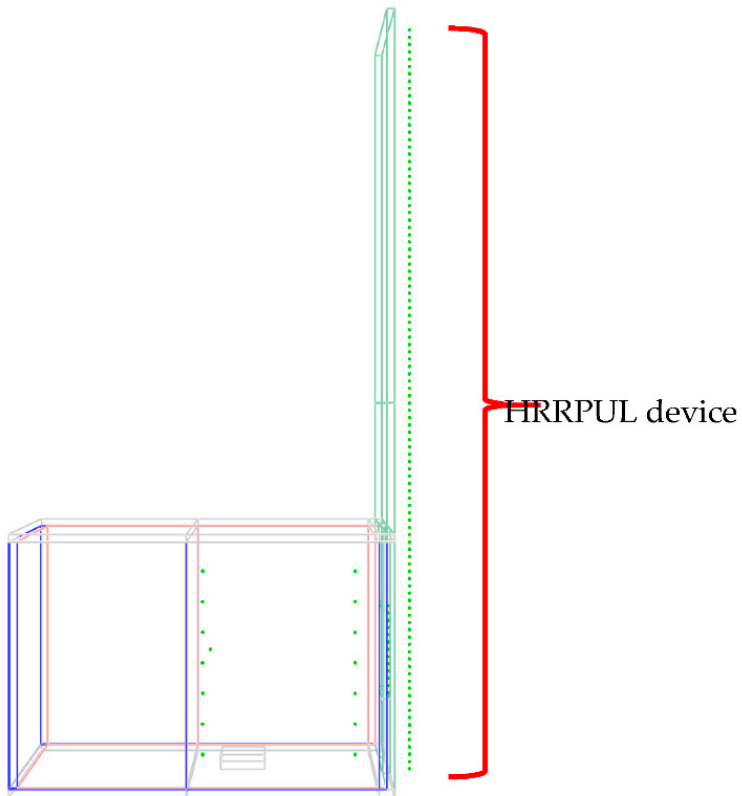

Figure 7. HRRPUL devices for flame height.

The wall material properties were defined as shown in Table 1 to accommodate heat losses through the walls and the ceiling. Furthermore, the auto-ignition temperature (AIT) of the propane gas was set at 450 °C to avoid any spurious combustion; it should be noted that the default setting in FDS modeling only considers fuel and oxygen mixture composition for ignition, and the mixture temperature is not taken into account [30].

Table 1. FDS wall materials input.

Parameter	Calcium Silicate Board	Ceramic Fiber Board	Cement Board
Density [kg/m^2]	250	18	1400
Specific heat [kJ/(kg·K)]	1.03	1.13	1.05
Conductivity [W/(m·K)]	0.05	0.8–0.22 (260–1093 °C)	0.36
Thickness [m]	0.0254	0.0127	0.006

Aside from specifying AIT, another important element that affects the simulation outcome is the grid size in the computational domain. A smaller grid size generally results in more accurate simulation, but requires a longer calculation time. To determine a proper grid size with a reasonable simulation time, a sensitivity analysis was performed using three different grid sizes—5 cm, 2.5 cm, and 1.25 cm—for the smallest (90 kW) and the largest (150 kW) fires. Two criteria were adopted to determine the proper grid size. The first is to determine whether there is any meaningful improvement in the parameters of interest by reducing the grid size, and the second is to determine the difference between the HRR output from the simulation and the input fire size. The results of 5 cm and 2.5 cm grid sizes presented considerable differences, as shown in Table 2; the difference ranged from 25% to 33% for the compartment gas temperature and 33% to 45% for the HRR inside the compartment. Then, the grid size was reduced from 2.5 cm to 1.25 cm and no substantial improvement was observed between these two grid sizes, although the 150 kW fire showed larger differences than the 90 kW fires. While 2.5 cm is still acceptable, 1.25 cm was selected for the grid size in the current study, promising more accurate results. The results from the sensitivity analysis are summarized in Table 2.

Table 2. Sensitivity analysis.

Fire Case	Parameters	1.25 cm Grid	2.5 cm Grid	5 cm Grid	% Difference—1.25 vs. 2.5	% Difference—2.5 vs. 5
90 kW with mid. opening	$\dot{Q}_{total}$ (kW)	88	87	80	1.1%	7.8%
	$\dot{Q}_{in}$ (kW)	55	54	30	0.5%	45%
	T_{in} (C)	975	968	652	0.7%	33%
	h_f (m)	0.8	0.9	0.9	13%	0%
150 kW with mid. opening	$\dot{Q}_{total}$ (kW)	149	148	140	0.9%	5.41%
	$\dot{Q}_{in}$ (kW)	49	45	30	8.3%	33%
	T_{in} (C)	947	896	676	5.4%	25%
	h_f (m)	1.2	1.35	1.3	13%	3.9%

2.3. Test Matrix

The test matrix is presented in Table 3. The comparison of the experimental and modeling results is expected to reveal unknowns in terms of airflow rates, HRRs inside and outside the compartment, and external flame height through a wall opening, using additional devices utilized in FDS. The name of each test or modeling is determined by the following conventions: E = (experiment); F = (FDS modeling), with the fire size in kW; opening elevation = (Bottom, Middle, and Top), based on Figure 4.

Table 3. Test Matrix.

Heat Release Rate (kW)	Experiment	FDS Modeling
90	E-90-Bot E-90-Mid E-90-Top	F-90-Bot F-90-Mid F-90-Top
110	E-110-Bot E-110-Mid E-110-Top	F-110-Bot F-110-Mid F-110-Top
130	E-130-Bot E-130-Mid E-130-Top	F-130-Bot F-130-Mid F-130-Top
150	E-150-Bot E-150-Mid E-150-Top	F-150-Bot F-150-Mid F-150-Top

2.4. Steady-State Data Extraction

Due to the heat transfer through the walls and the ceiling of the compartment and the relatively low-temperature ambient airflow into the compartment, the compartment gas temperature changes gradually. A preliminary experiment with a 150 kW fire was conducted to identify how to determine the steady-state temperature. With the ambient temperature ranging from 5 to 10 °C, the compartment needed to be preheated to reach a relatively steady temperature and heat release rate. Although propane gas was used as a fuel source, the fire was extinguished soon after ignition without preheating. Therefore, the propane fuel flow rate was gradually increased from 30 kW to 150 kW. The steady-state period was determined based on the HRR measured by the oxygen depletion calorimeter and the compartment temperature data from thermocouples. Only 600 s of steady-state data from 900 s to 1500 s were trimmed out and used for analysis in the experiment, as shown in Figure 8a,c. For FDS modeling, each simulation ran for 1000 s; steady-state data from 400 to 1000 s were trimmed out, and the average temperature was used for analysis.

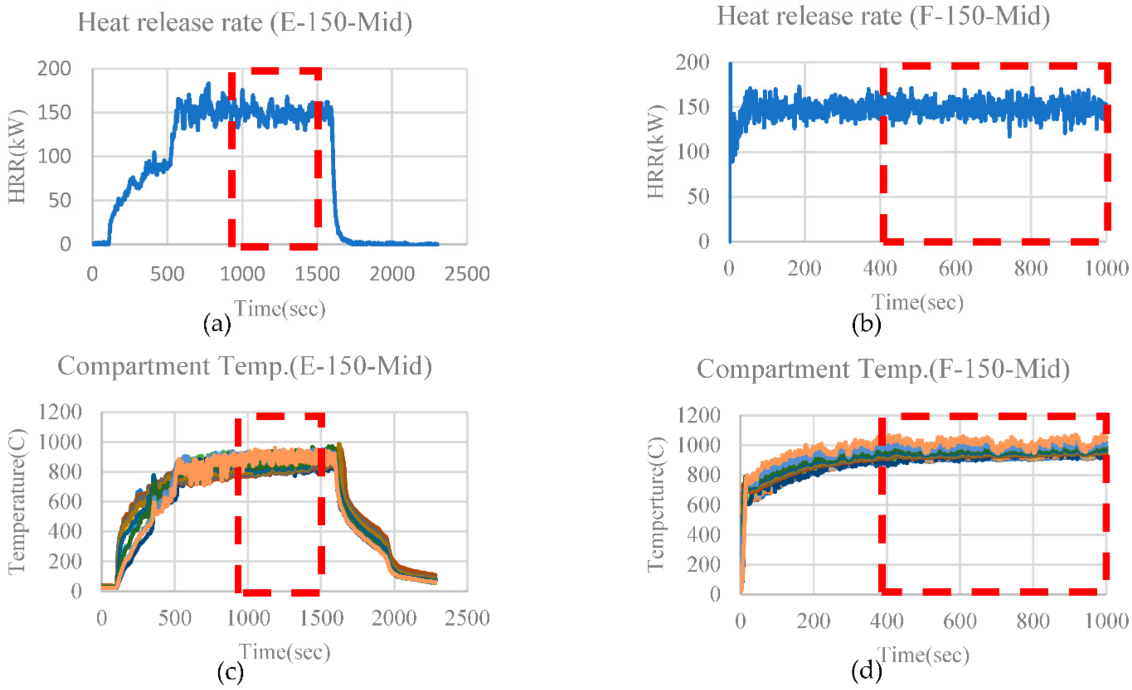

Figure 8. An example of data trimming for the steady-state; (**a**,**c**) are from the experiments, and (**b**,**d**) are from FDS modeling.

3. Results

This section presents the effect of the wall opening location on the compartment gas temperature and external flame height. Further investigation on the reasons for the different effects is conducted through FDS modeling.

3.1. Experiment Results

According to Equation (5) and the energy balance $\dot{Q}_{ex} = \dot{Q}_{total} - \dot{Q}_{in}$, all experimental cases having the same fuel flow rate are expected to have identical HRRs inside and outside the compartment. Since the HRRs inside and outside the compartment cannot be directly measured in experiments, the gas temperature within the compartment and external flame heights were measured to represent the HRRs inside and outside, respectively, and the results are presented in Figure 9. A higher gas temperature means a higher HRR inside the compartment, and a higher external flame height means a higher HRR outside the compartment.

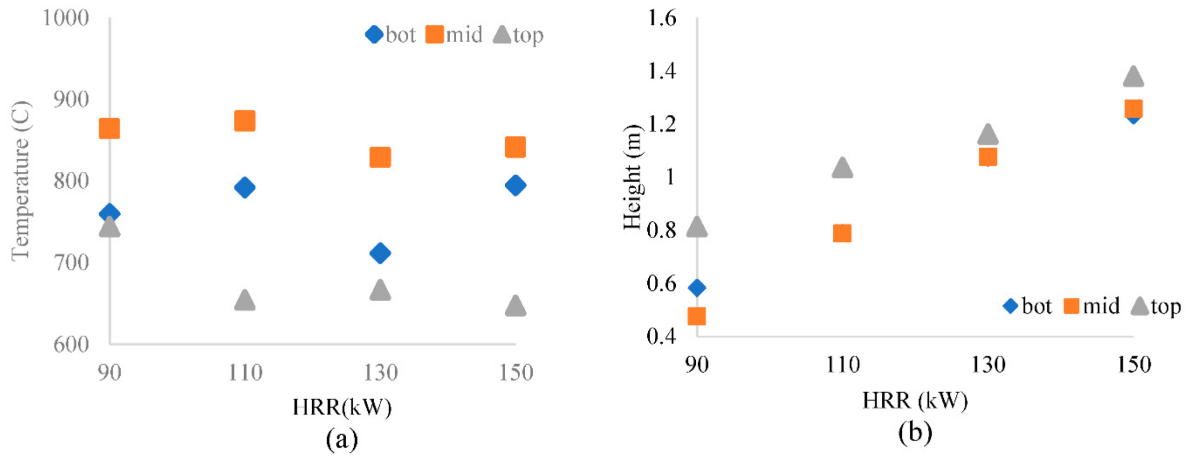

Figure 9. Experiment results: (**a**) gas temperature inside the compartment and (**b**) external flame height.

The gas temperatures inside the compartment varied as the opening location changed. With the same opening area and height, the experiments with the middle opening showed the highest gas temperature inside and those with the top opening showed the lowest temperature. The external flame heights also varied; the experiments with the top opening presented taller flame heights for all fire sizes and those with the middle and bottom opening showed relatively similar flame heights, although the bottom opening has a slightly higher flame height at a lower fire size (90 kW) and a slightly lower flame height at a higher fire size (150 kW). The gas temperature and external flame height data substantiated that varying wall opening locations can lead to different compartment fire phenomena. Among the three different wall opening elevations, the most gas fuel is burned inside with the middle opening and the least is burned with the top opening.

3.2. FDS Results and Analysis

The gas temperatures inside the compartment and the external flame heights of the FDS modeling results are compared to the experimental results to check if FDS outputs are reasonable for further investigation. The steady-state compartment gas temperature data from the experiments and the modeling are shown in Figure 10.

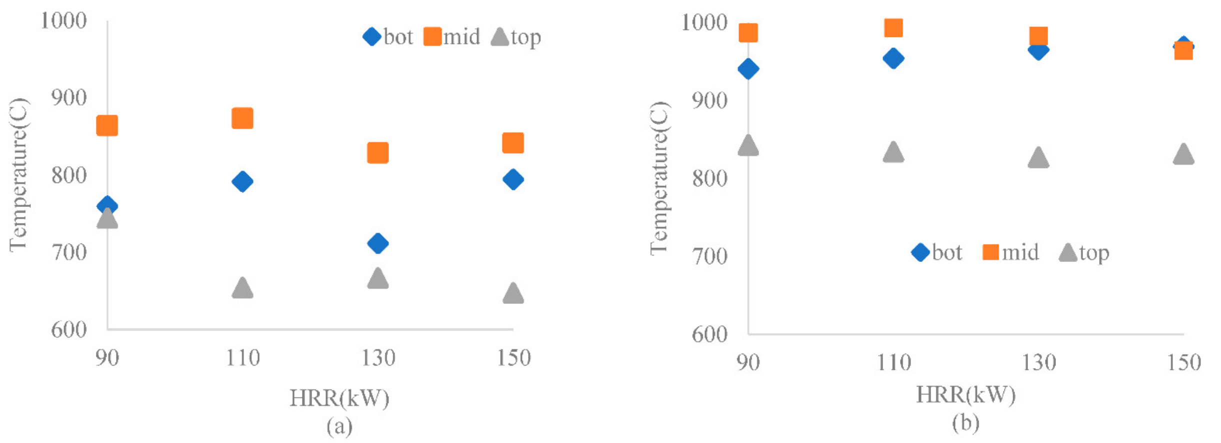

Figure 10. Comparison of the average compartment gas temperatures from (**a**) experiments and (**b**) FDS modeling.

The FDS modeling results are roughly about 150 °C higher than those from the experiments. There may be various reasons for this discrepancy, such as the material properties typed in the modeling which may not be accurate enough compared to those in the experiments. It may be also due to the increased convective heat loss on the compartment's exterior surface caused by make-up air for the exhaust hood in the lab during the experiments. In the FDS modeling, the ambient temperature was set at 5 °C, but any airflow around the compartment caused by exhaust, i.e., with natural convection only, was not implemented. Despite the temperature difference of about 150 °C, the results reveal a similar pattern of the compartment gas temperatures of the three opening locations; the average gas temperature with the middle opening is the highest, followed by those with the bottom and the top openings.

The external flame height was calculated based on the extracted images from the captured video clips from the experiments, while the HRRPUL device was used for FDS modeling. The external flame height was calculated from the neutral plane height, i.e., from the bottom of the flame outside the compartment. The results are presented in Figure 11. For the 90 kW and 110 kW fire cases, the flame heights in the experiments are slightly lower than those in the FDS modeling. This may be partially due to more fluctuating external flames at lower heat release rates; with sufficient unburned fuel gases leaving the compartment at 130 kW or 150 kW, more steady external flames were observed. This is congruent with a previous study demonstrating that the probability of capturing correct flame height is lower at lower HRRs [31]. Despite the discrepancy at lower HRRs, both experimental and modeling results show a similar pattern: the compartment with the top opening has the tallest external flame height followed by the middle and the bottom openings. This means there is more unburned fuel leaving the compartment with the top opening.

FDS provides a device to calculate an HRR value for a specific region in the modeling domain. The HRRs inside and outside the compartment were obtained from the FDS modeling as shown in Figure 12.

The middle opening presents the highest HRR inside the compartment, indicating that more combustion occurred inside the compartment. With the same amount of fuel provided, this also means the amount of air reacting with the fuel in the compartment was larger. The top opening presents the highest HRR and the tallest flame height outside the compartment, indicating that less air is reacted inside the compartment, leading to more unburned fuel escaping and combusted outside.

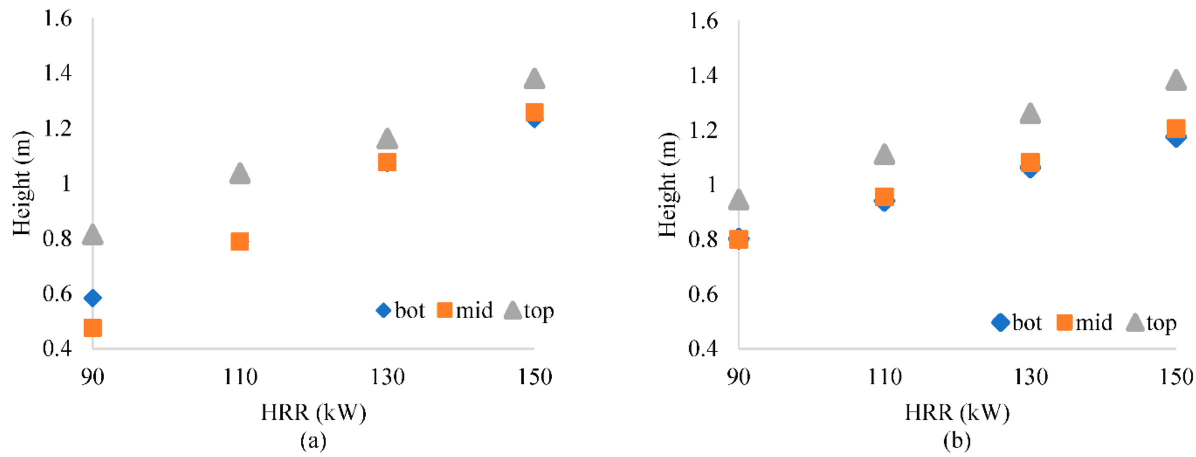

Figure 11. Comparison of the external flame heights from (**a**) experiments and (**b**) FDS modeling.

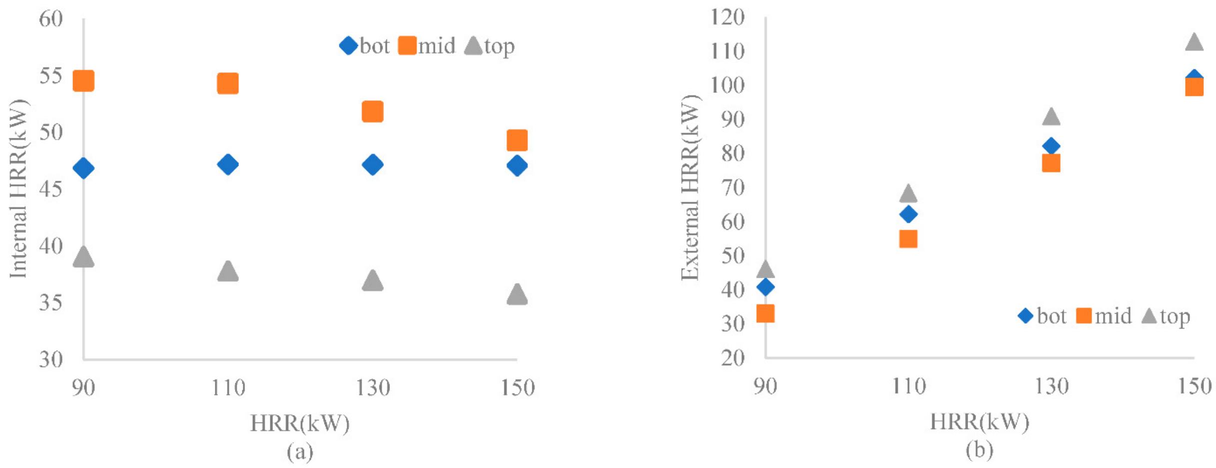

Figure 12. (**a**) HRR inside the compartment and (**b**) HRR outside the compartment from FDS modeling.

4. Discussion

Both the experiment and modeling results show that the wall opening location influenced the compartment fire behavior. With the bottom, middle, and top opening, the results showed the following trends, as presented in Table 4.

Table 4. The effect of wall opening elevation on the various parameters of compartment fires and external flame height.

	Trend
Compartment gas temperature	$T_{in\_mid} > T_{in\_bot} > T_{in\text{-}top}$
HRR inside the compartment	$Q_{in\_mid} > Q_{in\_bot} > Q_{in\_top}$
HRR outside the compartment	$Q_{ex\_mid} < Q_{ex\_bot} < Q_{ex\_top}$
External flame height	$h_{f\_mid} \approx h_{f\_bot} < h_{f\_top}$

One of the fundamental reasons for this difference is the amount of air reacting with the fuel inside the compartment, which can be influenced by the flow paths of fresh air into the compartment. To visually analyze the flow paths, representative snapshots of the velocity vector from 130 kW fires are included in Figure 13. The bottom opening provides the incoming air with a straight path and the shortest travel distance to the fuel source, which allows for more flames at the back of the compartment. The top opening offers the incoming air with the longest travel distance to the fuel source in a downward direction, and the buoyancy of combustion products competes with the incoming airflow, which may result in its entrainment to the outflow without meeting fuel gas. The compartment with a middle opening presents a stronger fuel–air mixture; the area showing dynamic flow motion near the opening is larger than those of the other openings, with higher velocities.

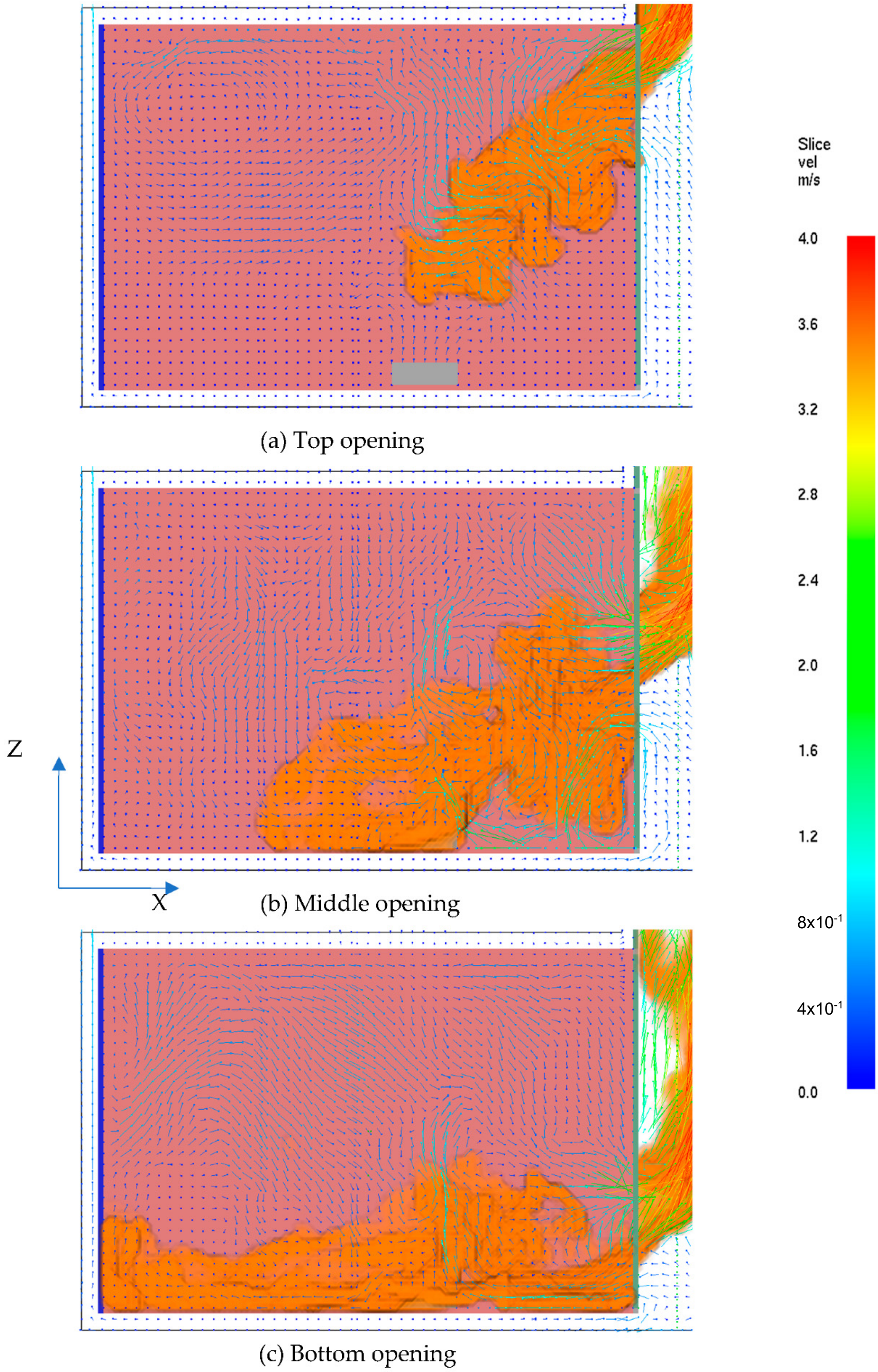

Figure 13. FDS velocity vector slices at Y = 0.4 m, dissecting the opening in half, captured at 800 s in a 1.2 m deep (X = 1.2) and 0.8 m high (Z = 0.8) compartment.

The cause of the different amounts of air involved in combustion within the compartment may be understood according to two aspects—the air inflow amount and the combustion efficiency. Either one of these, or both, can change the amounts. In most experimental studies of compartment fire phenomena, the former is often assumed to be identical, as shown in Equation (4), and the latter is often checked by comparing the amount of fuel flow rate multiplied by the heat of combustion and the heat release rate measured by the oxygen consumption calorimeter. In the current study, two factors (factor K and factor O) are introduced to quantify their effect on the amount of air involved in the combustion reaction within the compartment.

4.1. Factor K

To address the difference in the flow rate of air into the compartment, factor K, as shown in Equation (6), is introduced. It indicates the ratio of air that enters the compartment in FDS modeling to the value based on the existing Equation (4).

$$K = \frac{\dot{m}_{air\_FDS}}{\dot{m}_{a\_Eq}} \tag{6}$$

where, $\dot{m}_{a\_Eq} = 0.5A_o\sqrt{H_o}$.

Factor K varies with the wall opening location, and the values for multiple fire sizes are presented in Figure 14a. Factor K ranges from 78% to 95% of the value of Equation (4). The middle opening allows about 10% more air than the other two opening locations. More air in the compartment led to higher gas temperatures, as substantiated by the experiments and HRRs inside the compartment, as shown in FDS modeling.

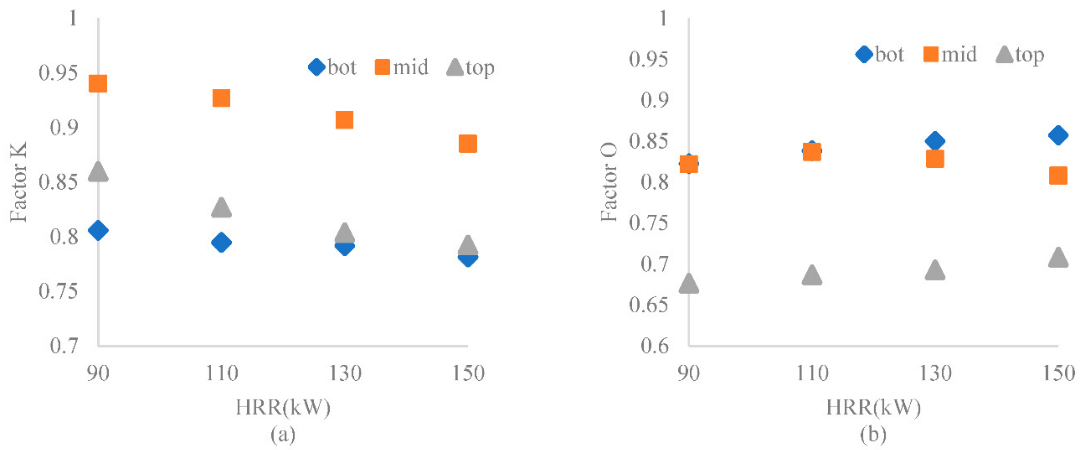

Figure 14. (**a**) Factor K and (**b**) factor O for various compartment fire sizes and wall opening elevations.

4.2. Factor O

Besides the varying mass flow rates of air into the compartment, the percent of oxygen burned in the compartment may be another reason for different inside HRRs. It is often assumed that the air entering the compartment is completely consumed, but if the amount of oxygen is less than the limiting oxygen concentration, combustion is not possible. FDS uses 13.5 Vol% as a default [29]. Based on the HRR inside, the mass consumption rate of oxygen is calculated as Equation (7).

$$\dot{m}_{o_2\_consumed} = \frac{\dot{Q}_{in}}{13,100\ \mathrm{kJ/kg}} \tag{7}$$

To indicate the contribution of oxygen to the HRR inside, factor O, the ratio of oxygen consumed for combustion to the oxygen entering the compartment, is defined as shown in Equation (8).

$$O = \frac{\dot{m}_{O_2\_consumed}}{\dot{m}_{O_2\_\mathrm{inflow}}} = \frac{\dot{Q}_{in}}{(13,100\ \mathrm{kJ/kg})\dot{m}_{O_2\_\mathrm{inflow}}} \tag{8}$$

The values of factor O are presented in Figure 14b. Approximately 80% to 85% of oxygen coming into the compartment was consumed in the compartment with the bottom or the middle opening. The compartment with the top opening has a significantly lower factor O, at about 67%. This may be due to a larger fraction of air inflow entrained to the outflow; it should be noted that the amount of air entering the compartment with the top and the bottom opening are similar as shown in Figure 14a.

4.3. Updated Mass Flow Diagram for a Compartment Fire

It is often assumed that all the inflow is fresh air, but the FDS mass flow devices showed that $\dot{m}_a \neq \dot{m}_{\text{inflow}}$. Based on FDS modeling, strictly speaking, about 1–2% of the inflow (noted as α in Figure 15) is composed of combustion products and unburned fuels, which are entrained from the outflow to the inflow back to the compartment. In addition, the air entering the compartment in the inflow was not all involved with combustion: about 15%~35% of the air inflow was entrained to the outflow. This is indicated as β in Figure 15. With the default oxygen mass fraction in FDS, y_{O_2}= 0.230997, the mass flow rate of oxygen into the compartment is calculated as $y_{O_2} \cdot K \cdot \dot{m}_{a\_Eq}$. Combined with factor O, the rate of oxygen consumption is written as $O \cdot y_{O_2} \cdot K \cdot \dot{m}_{a\_Eq}$. Therefore, the HRR inside the under-ventilated compartment in Equation (5) is updated to Equation (9), and the compartment fire flow diagram is updated as Figure 15.

$$\dot{Q}_{in} = 13,100 \cdot y_{O_2} \cdot \dot{m}_{a\_Eq}(K \cdot O) \tag{9}$$

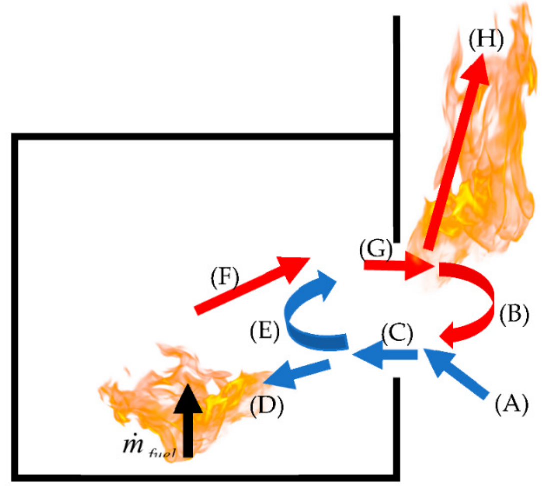

$(A): \dot{m}_{air\_FDS} = K \cdot \dot{m}_{a\_Eq}$

$(B): \dot{m}_{entrained\_\text{inflow}} = \alpha \cdot \dot{m}_{\text{outflow}}$

$(C): \dot{m}_{\text{inflow}} = \dot{m}_{air\_FDS} + \dot{m}_{entrained\_\text{inflow}}$

$(D): \dot{m}_{O_2\_consumed} = O \cdot y_{O_2} \cdot K \cdot \dot{m}_{a\_Eq}$

$(E): \dot{m}_{air\_\text{outflow}} = \beta \cdot \dot{m}_{air\_FDS}$

$(F): \dot{m}_{unburned\ fuel} + \dot{m}_{combustion\ products}$

$(G): \dot{m}_{\text{outflow}} = \dot{m}_{unburned\ fuel} + \dot{m}_{combustion\ products} + \dot{m}_{air\_\text{outflow}}$

$(H): \dot{m}_{external} = \dot{m}_{\text{outflow}} - \dot{m}_{entrained\_\text{inflow}}$

Figure 15. The mass flow diagram in a compartment fire determined by FDS.

Equation (9) shows that the compartment fire and external flame phenomena are influenced by not only the ventilation factor, but also by the amount of oxygen entering and burning in the compartment as a function of the opening location. These two are represented by factors K and O. Since the multiplied values of K and O vary from 0.55 to 0.77, as shown in Figure 16, the existing correlation for the HRR inside the compartment is found to be overestimated.

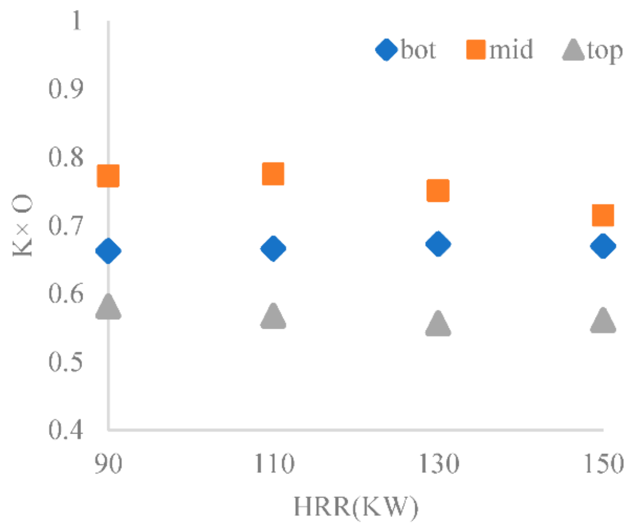

Figure 16. K multiplied by O, indicating the ratio of the air entering and reacting with fuel in the compartment, as determined by FDS to $\dot{m}_a \approx 0.5A_o\sqrt{H_o}$.

5. Conclusions

From the fire engineering perspective, the top opening presents higher fire spread hazards to the upper floors. Not only is the opening closer to the upper floors, but it also generates a larger external fire with a taller flame height. The wall opening location has not been well perceived as an independent variable for the compartment fire phenomena in under-ventilated conditions and associated projected flame out of the opening. However, it is found that the wall opening location affects the amount of incoming and outgoing gas flows, leading to varying combustion efficiencies within the compartment. To account for these variations, two factors are introduced in the current study based on FDS modeling.

Factor K indicates the amount of air entering the compartment relative to the existing correlation ($0.5A_o\sqrt{H_o}$). The middle wall opening allows for about 10% more air inflow than the top and bottom openings.

Factor O indicates that not all the air entering the compartment is reacted with fuel. Depending on the wall opening location, it is found that about 15–35% of air inflow is entrained to the outflow, and is not used for combustion reaction within the compartment.

Based on the factor K and O values for the compartment and opening dimensions given in this study, the existing correlations for the mass flow rate of air into the compartment ($0.5A_o\sqrt{H_o}$) and the maximum HRR inside the compartment ($1500A_o\sqrt{H_o}$) may be overestimated by about 6–22% and 15–33%, respectively. It should be noted that these variations are based on the FDS modeling results. Further studies are required to develop generalized correlations that include the wall opening location as an independent variable. A comparative study with real-scale compartment and computer modeling would also be beneficial, as this would be expected to minimize any scaling effect on the results.

Author Contributions: Conceptualization, H.P.; Data curation, L.W.; Formal analysis, L.W.; Investigation, L.W. and H.P.; Methodology, H.P.; Supervision, H.P.; Writing—original draft, L.W.; Writing—review & editing, H.P. All authors have read and agreed to the published version of the manuscript.

Funding: This research received no external funding.

Conflicts of Interest: The authors declare no conflict of interest.

Nomenclature

A_o	Opening area (m^2)
C_d	Drag coefficient
d_f	Density factor
g	Gravitational acceleration (m/s^2)
h_1	Neutral plane height from the bottom of the opening (m)
h_f	External flame height (m)
H_o	Opening height (m)
$\dot{m}_g$	Mass flow rate of combustion products out of the compartment (kg/s)
$\dot{m}_a$	Mass flow rate of air into the compartment (kg/s)
$\dot{m}_{a\_Eq}$	Mass flow rate of air into the compartment based on existing equations (kg/s)
$\dot{m}_{air\_FDS}$	Mass flow rate of air into the compartment, determined by FDS (kg/s)
$\dot{m}_{air\_outflow}$	Mass flow rate of unreacted air leaving the compartment (kg/s)
$\dot{m}_{combustion\ products}$	Mass flow rate of combustion products leaving the compartment, including nitrogen (kg/s)
$\dot{m}_{entrained\_\mathrm{inflow}}$	Mass flow rate of entrained gases to the inflow from the outflow (kg/s)
$\dot{m}_{entrained\_air\_\mathrm{outflow}}$	Mass flow rate of entrained air to the outflow from the inflow (kg/s)
$\dot{m}_{external}$	Net mass flow rate of gases contributing to external flame (kg/s)
$\dot{m}_{\mathrm{inflow}}$	Mass flow rate of gases entering the compartment (kg/s)
$\dot{m}_{O_2\_consumed}$	Mass consumption rate of oxygen (kg/s)
$\dot{m}_{O_2\_\mathrm{inflow}}$	Mass flow rate of oxygen into the compartment, determined by FDS (kg/s)
$\dot{m}_{outflow}$	Mass flow rate of gases leaving the compartment (kg/s)
$\dot{m}_{unburned\ fuel}$	Mass flow rate of unburned fuel leaving the compartment (kg/s)
$\dot{Q}_c$	Critical heat release rate inside the compartment (kW)
$\dot{Q}_{in}$	Heat release rate inside the compartment, determined by FDS (kW)
$\dot{Q}_{total}$	Total heat release rate (kW)
$\dot{Q}_{ex}$	Heat release rate outside the compartment, determined by FDS (kW)
T_a	Ambient air temperature (K)
T_g	Upper gas layer temperature in the compartment (K)
T_{in}	Average gas temperature in the compartment(K)
W_o	Opening width (m)
y_{O_2}	Mass fraction of oxygen in the air
α	Fraction of $\dot{m}_{entrained\_\mathrm{inflow}}$ to $\dot{m}_{outflow}$
β	Fraction of $\dot{m}_{air\_\mathrm{ouflow}}$ to $\dot{m}_{air\_FDS}$
ρ_a	Ambient air density (kg/m^3)
ρ_g	Density of gases in the compartment (kg/m^3)

References

1. Utiskul, Y.; Quintiere, J.G.; Rangwala, A.S.; Ringwelski, B.A.; Wakatsuki, K.; Naruse, T. Compartment fire phenomena under limited ventilation. *Fire Saf. J.* **2005**, *40*, 367–390. [CrossRef]
2. Delichatsios, M.A.; Silcock, G.W.; Liu, X.; Delichatsios, M.; Lee, Y.-P. Mass pyrolysis rates and excess pyrolysate in fully developed enclosure fires. *Fire Saf. J.* **2004**, *39*, 1–21. [CrossRef]
3. Yokoi, S. *Study on the Prevention of Fire-Spread Caused by Hot Upward Current*; BRI Report; Building Research Institute, Ministry of Construction of Japan: Tokyo, Japan, 1960; p. 34.
4. Ren, F.; Zhang, X.; Hu, L.; Sun, X. An experimental study on the effect of fire growth in a lower-floor compartment on fire evolution and facade flame ejection from an upper-floor compartment. *Proc. Combust. Inst.* **2019**, *37*, 3909–3917. [CrossRef]
5. Lee, Y.-P.; Delichatsios, M.A.; Silcock, G.W.H. Heat fluxes and flame heights in façades from fires in enclosures of varying geometry. *Proc. Combust. Inst.* **2007**, *31*, 2521–2528. [CrossRef]
6. Lee, Y.-P.; Delichatsios, M.; Ohmiya, Y. The physics of the outflow from the opening of an enclosure fire and re-examination of Yokoi s correlation. *Fire Saf. J.* **2012**, *49*, 82–88. [CrossRef]
7. Lee, Y.-P.; Delichatsios, M.A.; Ohmiya, Y. The study for the physics of the outflow from the opening of a burning enclosure. In Proceedings of the 5th International Seminar on Fire and Explosion Hazards, Citeseer, Edinburgh, UK, 23–27 April 2007; p. 27.
8. Himoto, K.; Tsuchihashi, T.; Tanaka, Y.; Tanaka, T. Modeling thermal behaviors of window flame ejected from a fire compartment. *Fire Saf. J.* **2009**, *44*, 230–240. [CrossRef]
9. Quintiere, J.G.; Cleary, T.G. Heat flux from flames to vertical surfaces. *Fire Technol.* **1994**, *30*, 209–231. [CrossRef]
10. Karlsson, B.; Quintiere, J.G. *Enclosure Fire Dynamics*; CRC Press: Boca Raton, FL, USA, 2000.

11. Huggett, C. Estimation of rate of heat release by means of oxygen consumption measurements. *Fire Mater.* **1980**, *4*, 61–65. [CrossRef]
12. Johansson, N.; Van Hees, P. A Simplified Relation Between Hot Layer Height and Opening Mass Flow. *Fire Saf. Sci.* **2014**, *11*, 432–443. [CrossRef]
13. Tang, F.; Hu, L.; Qiu, Z.W.; Zhang, X.; Lu, K. Window ejected flame height and heat flux along facade with air entrainment constraint by a sloping facing wall. *Fire Saf. J.* **2015**, *71*, 248–256. [CrossRef]
14. Huang, H.; Ooka, R.; Liu, N.; Zhang, L.; Deng, Z.; Kato, S. Experimental study of fire growth in a reduced-scale compartment under different approaching external wind conditions. *Fire Saf. J.* **2009**, *44*, 311–321. [CrossRef]
15. Ren, F.; Hu, L.; Sun, X.; Hu, K. An experimental study on vertical temperature profile of facade fire plume ejected from compartment with an opening subjected to external wind normal to facade. *Int. J. Therm. Sci.* **2018**, *130*, 94–99. [CrossRef]
16. Zhang, X.; Zhang, Z.; Zhang, Z.; Xu, W.; Luo, Q.; Tao, H.; Li, X. Experimental investigation of compartment fires with circular opening: From the aspects of internal temperature and facade flame. *Combust. Flame* **2020**, *213*, 107–116. [CrossRef]
17. Delichatsios, M.A.; Lee, Y.-P.; Tofilo, P. A new correlation for gas temperature inside a burning enclosure. *Fire Saf. J.* **2009**, *44*, 1003–1009. [CrossRef]
18. Sun, X.; Hu, L.; Yang, Y.; Ren, F.; Fang, X. Evolutions of gas temperature inside fire compartment and external facade flame height with a casement window. *J. Hazard. Mater.* **2020**, *381*, 120913. [CrossRef]
19. Sun, X.; Hu, L.; Zhang, X.; Ren, F. Experimental study on evolution of compartment fire and facade flame through an opening with the fire source attached to a backwall at different elevations. *Proc. Combust. Inst.* **2019**, *37*, 3919–3926. [CrossRef]
20. Snegirev, A.Y.; Makhviladze, G.M.; Talalov, V.A.; Shamshin, A.V. Turbulent Diffusion Combustion under Conditions of Limited Ventilation: Flame Projection through an Opening. *Combust. Explos. Shock Waves* **2003**, *39*, 1–10. [CrossRef]
21. Takeda, H.; Akita, K. Critical phenomenon in compartment fires with liquid fuels. *Symp. (Int.) Combust.* **1981**, *18*, 519–527. [CrossRef]
22. Tang, F.; Hu, L.; Delichatsios, M.A.; Lu, K.; Zhu, W. Experimental study on flame height and temperature profile of buoyant window spill plume from an under-ventilated compartment fire. *Int. J. Heat Mass Transf.* **2012**, *55*, 93–101. [CrossRef]
23. Frank, K.; Park, H.; Baker, G.; Wade, C. *SR360 Vertical External Fire Spread from Flames Extending out of an Opening*; Study Report; BRANZ; Ministry of Business Innovation & Employment: Wellington, New Zealand, 2018.
24. Lu, K.; Wang, Z.; Ding, Y.; Wang, J.; Zhang, J.; Delichatsios, M.A.; Hu, L. Flame behavior from an opening at different elevations on the facade wall of a fire compartment. *Proc. Combust. Inst.* **2020**, *38*, 4551–4559. [CrossRef]
25. Hu, L.; Liu, S.; Xu, Y.; Li, D. A wind tunnel experimental study on burning rate enhancement behavior of gasoline pool fires by cross air flow. *Combust. Flame* **2011**, *158*, 586–591. [CrossRef]
26. Hu, L.; Liu, S.; Wu, L. Flame radiation feedback to fuel surface in medium ethanol and heptane pool fires with cross air flow. *Combust. Flame* **2013**, *160*, 295–306. [CrossRef]
27. Fleischmann, C.; Parkes, A. Effects Of Ventilation On The Compartment Enhanced Mass Loss Rate. *Fire Saf. Sci.* **1997**, *5*, 415–426. [CrossRef]
28. Yang, D.; Hu, L.; Jiang, Y.Q.; Huo, R.; Zhu, S.; Zhao, X. Comparison of FDS predictions by different combustion models with measured data for enclosure fires. *Fire Saf. J.* **2010**, *45*, 298–313. [CrossRef]
29. McGrattan, K.B. *Fire Dynamics Simulator (Version 6): Technical Reference Guide*; National Institute of Standards and Technology: Gaithersburg, MD, USA, 2021.
30. McGrattan, K.B.; Forney, G.P. *Fire Dynamics Simulator (Version 6): User's Guide*; National Institute of Standards and Technology: Gaithersburg, MD, USA, 2021.
31. Hu, L.; Lu, K.; Delichatsios, M.; He, L.; Tang, F. An experimental investigation and statistical characterization of intermittent flame ejecting behavior of enclosure fires with an opening. *Combust. Flame* **2012**, *159*, 1178–1184. [CrossRef]